Engineering Structures 299 (2024) 117090

Contents lists available at ScienceDirect

Engineering Structures

journal homepage: www.elsevier.com/locate/engstruct

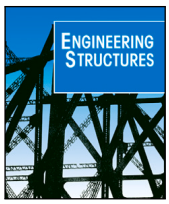

Railway catenary optimisation with span variability by an iterative optimisation algorithm for large numbers of parameters

J. Gil [a,*], Y. Song [b], S. Gregori [a], M. Tur [a], A. Rønnquist [b], F.J. Fuenmayor [a]

[a] Instituto de Ingeniería Mecánica y Biomecánica, Universitat Politècnica de València, Camino de Vera s/n, 46022, Valencia, Spain
[b] Department of Structural Engineering, Norwegian University of Science Technology NTNU, Trondheim, Norway

ARTICLE INFO

Keywords:
Catenary
Pantograph
Optimisation
Experimental validation

ABSTRACT

Optimising the catenary topology to improve the pantograph–catenary interaction is computationally expensive. Especially in the case of large numbers of parameters. Unfortunately, varying span lengths and dropper distribution in realistic systems requires the inclusion of a vast number of parameters, making the optimisation problem extremely complicated. Published optimisation works assume that the catenary is a perfectly periodical structure to reduce the number of parameters involved in the optimisation and keep the computational cost below a feasible limit. This paper attempts to deal with the scientific challenge of optimising a realistic system by proposing an iterative optimisation strategy consisting of optimising groups of parameters separately and repeating the optimisations iteratively to consider the dependence between parameters that otherwise would need to be optimised together. This solution performs topological catenary optimisation in catenary zones with span variability or transition zones in which optimisations that assume periodicity are no longer valid.

1. Introduction

1.1. Background

A substantial proportion of railway lines are electrified and the number has been growing since the start of the present trend in clean energies. The most frequently used system in electrified lines is that of Overhead Contact Lines (OCL), or catenaries. Every train that obtains electric current from catenaries is furnished with at least one pantograph that keeps sustained sliding contact with the catenary. The higher the speed train travels, the more unfavourable conditions for the pantograph–catenary system, and the more likely loss of contact becomes. The primary mechanism for avoiding loss of contact is the uplift system, which raises the contact force between the pantograph and catenary, but unfortunately it also increases the wear and maintenance costs. Improving the pantograph–catenary system by other means is therefore crucial for increasing running speeds and enhancing the durability of the catenaries.

Various approaches can be used for investigating at pantograph–catenary system [1], while nowadays most of them rely on numerical simulations to evaluate the system performance, at least in the early stages of the design process, due to the high availability of numerical simulation tools that allow the virtual recreation of the pantograph–catenary dynamic interaction with accurate models, low cost and complete observability. The most popular catenary models used in numerical simulations are built by the Finite Element Method and a comprehensive collection of these pantograph–catenary models can be found in [2].

Numerical simulations are essential for conducting computational optimisation of the different parameters that participate in the problem. Essentially, they can be divided into pantograph optimisations and catenary optimisations. The work conducted in [3] assesses the influence of different parameters in the current collection quality and concludes that stiffness and damping of the pantograph head and frame, uplift force and contact wire tension are closely related to the dynamic behaviour of the system. Other parameters affecting the catenary, such as pre-sag [4] or dropper spacing [5] have been shown to be relevant in catenary optimisation. Several successful optimisations of the pantograph models can be found in the literature, for instance in [6], the parameters of a lumped pantograph model are optimised, or in [7] a pneumatic suspension is used to improve pantograph performance coupled with the catenary. Also, some authors have attempted to optimise the catenary designs as described in Section 1.3.

There is now a vast quantity of optimisation algorithms that can be used to find the best parameters related to the problem. The study [8] provides a good insight into the different methods and includes derivative-based, metaheuristic, and surrogate-based methods, among others. The ever-increasing computational power allows more ambitious optimisation problems with more optimisation parameters.

* Corresponding author.
E-mail address: jaigiro@upv.es (J. Gil).

https://doi.org/10.1016/j.engstruct.2023.117090
Received 17 June 2023; Received in revised form 19 September 2023; Accepted 22 October 2023
Available online 2 November 2023

1.2. Problem of interest

While the pantograph–catenary system can be improved by optimising the different systems participating in the problem, the present work focuses on optimising the catenary. The first step for this is to create a computational model that relates the catenary design parameters to a performance indicator or objective function. In every optimisation problem, the objective function must be evaluated many times for the different parameter combinations. The higher the number of parameters, the higher the number of evaluations.

In the pantograph–catenary interaction problems, every evaluation entails solving the initial configuration problem and the dynamic interaction problem. The first of these consists of solving a non-linear equation system with a large number of variables or degrees of freedom (10 000–20 000 per km) and provides the initial position of the catenary. The second consists of integrating the pantograph and catenary dynamic equations and is also non-linear, since dropper slackening is involved. In short, evaluating the objective function is computationally expensive and this factor limits the number of parameters that can be optimised.

The catenary design parameters can be divided into global and local. The former are those that affect the entire catenary, such as the wire tension or mass. Local parameters are those that affect a specific area in the catenary, such as the length or position of the droppers. However, local parameters can become global if periodicity is considered, which means that the catenary spans are equal and every parameter affects all the others. The studies on catenary optimisation in the literature only include a few parameters and when local parameters are included they assume periodicity and symmetry in the span configuration. The present study is aimed to optimise the local parameters in a real catenary design with varying span length, thus ruling out the assumption of periodicity. In this scenario, a large number of parameters need to be optimised, which is prohibitive to optimise all at once in terms of computational cost. Local parameters were thus optimised iteratively, taking advantage of the reduced influence zone of each parameter to define a proper optimisation strategy.

1.3. Literature review

In the literature there is an endless list of different optimisation methods and in recent years the use of intelligent computational methods has become more popular. The book [9] contains a collection of intelligent approaches such as evolutionary algorithms, swarm algorithms and neural network computing. Additionally, the methods are applied for different structural optimisation problems to improve the topology and materials. Besides the boundless number of structural optimisations that can be found, this section reviews the different alternatives that have been used for optimising catenary designs in the last few years.

In [10], the speed limit of an existing catenary design is increased by 23%, changing the tension of the messenger and contact wire and the pre-sag. In that work, the contact wire dynamic response and uplift are considered to evaluate the speed limit of the catenary and the effect of the changing parameters. The work [11] studies not only the tensions of the messenger and contact wire but also the mass of both wires and includes a sensitivity analysis of the parameters in the contact force standard deviation by central composite design and optimisation at a speed of 500 km/h. In [12], in contrast to the previous works, the topological optimisation is investigated, allowing the contact wire to have different shapes to the conventional pre-sag. In that work, the optimisation parameters are the length and spacing of the catenary droppers, symmetry of the span arrangement and periodicity are assumed (leading to a number of parameters close to ten), the Genetic Algorithm is employed and the objective function is the contact force standard deviation. The optimum configurations found present a remarkable improvement, showing that the catenary topology has a significant influence on the problem. In [13], both catenary and pantograph optimisation are conducted in independent studies (not optimising parameters of both systems at once), but in this review we address only the catenary optimisation. Similarly to [12], in [13] dropper length and spacing are optimised, considering symmetry and periodicity but also the tension of the messenger and contact wires. In the work, non-dominated sorting genetic algorithm-II is used to avoid repeating the FEM simulation, while the objective function is the standard deviation and the mean of the contact force. It is worth noticing that in [13] the optimised catenary performs better in the 100–180 km/h range, even though it was optimised at the single speed of 160 km/h, showing a certain robustness of the results. In [14], the genetic algorithm is also used for the optimisation process, but in this case a surrogate model is used to reduce the computational cost of evaluating the objective function. This surrogate model is built by training a Back Propagation Neuronal Network. In that work, three independent optimisations are performed for the catenary to reduce the number of parameters per optimisation, splitting them into dropper spacing, dropper length and wire tensions. A significant improvement is found, with slight differences between the FEM simulations and the surrogate models used in the optimisations. To conclude, the study conducted in [15] uses Bayesian optimisation to improve the profile of the contact wire within the overlap sections, which are the most critical zones of the catenary as regards the current collection quality.

1.4. Scope and contributions

The scope of this paper is the modelling of a real catenary design, a comparison of the numerical simulation with experimental data, the topological optimisation of a whole section of the catenary and the analysis of the optimisation results.

Previous works on optimisation studied the parameters that have an overall effect on the catenary, while the present work focuses on parameters with local effect: i.e. the position and length of every individual dropper of the catenary. This optimisation modifies the topology of the entire catenary without assuming periodicity or span symmetry in order to satisfy the transitory design of certain of its parts. The biggest challenge in this approach is the large number of parameters to be optimised. The paper contribution is that it offers an alternative strategy for avoiding the prohibitive computational cost of optimisation by conventional methods. The strategy proposed entails sub-optimisations of reduced groups of parameters while leaving the remainder unaltered. These sub-optimisations were carried out on all the parameter groups and repeated iteratively until convergence. This strategy leads to much fewer evaluations of the objective function than the conventional approach and optimises all the parameters at once.

1.5. Organisation of the paper

The remainder of this paper is organised as follows. Section 2 describes the modelling of the pantograph–catenary dynamic interaction. In Section 3, the experimental measurements are contrasted with numerical simulations to validate the models. Section 4 describes the proposed optimisation method and Section 5 gives the results of the optimisation of a real catenary design, while Section 6 gives the paper main conclusions.

2. Modelling of the pantograph–catenary interaction

The catenary can be optimised thanks to the ability to evaluate the performance of different configurations by computational methods. It is therefore necessary to obtain computational models of the catenary and pantograph to compute their dynamic interaction and assess their performance. The pantograph–catenary dynamic interaction model used in this work only considers purely mechanical effects. Other types of actions (electromagnetic, wind on the catenary, movement of the pantograph's base, etc.) have not been considered.

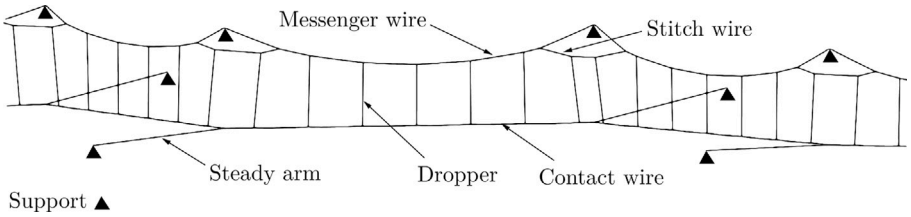

Fig. 1. Parts of the catenary FEM model.

2.1. Catenary model

In this work, from the different types of catenary we selected a stitched catenary, consisting of a contact wire, messenger wire, droppers, steady arms and stitch wires, as shown in Fig. 1. The Finite Element Method (FEM) is used to model the different wires and bars, employing ANCF (Absolute Nodal Coordinate Formulation) elements [16] for the contact, messenger and stitch wires and elements bar for the steady arms and droppers.

The catenary is subjected to gravity, which produces large displacements of the wires, defined by the degrees of freedom of the catenary nodes $\mathbf{q}$. This problem is governed by non-linear static equilibrium equations:

$$\mathbf{F}_{\text{int}}(\mathbf{q}) + \mathbf{F}_{\text{g}} = 0 \tag{1}$$

in which $\mathbf{F}_{\text{int}}$ and $\mathbf{F}_{\text{g}}$ are the internal elastic forces and the gravity forces, respectively. Additionally, the displacements of specific nodes in the deformed configuration must fulfil design requirements, for which the positions of the contact wire joints with droppers and steady arms are imposed. To satisfy these constraints, the lengths of some elements $\mathbf{l}$ need to be considered as unknowns. The initial configuration or 'shape-finding' problem consists of finding the position of the nodes and the lengths of droppers that satisfy both the static equilibrium and the design requirements:

$$\begin{aligned} &\mathbf{F}_{\text{int}}(\mathbf{q}, \mathbf{l}) + \mathbf{F}_{\text{g}}(\mathbf{l}) = 0 \\ &\mathbf{q}_c - \mathbf{P} = 0 \end{aligned} \tag{2}$$

in which $\mathbf{q}_c$ are the node degrees of freedom which are constrained by the design, and $\mathbf{P}$ are the positions imposed for these nodes. Additionally, specific tensions of some wires can be required and restriction equations for the tensions must be included. A comprehensive description of this problem can be found in [17], from which the methodology was taken for the present study.

Once the initial configuration problem is solved, the dynamic interaction of the catenary with the pantograph can be computed. In this dynamic problem small displacement theory is considered, and the non-linear formulation of the FEM model of the catenary can be linearised around the equilibrium point $\mathbf{q}_0$:

$$\begin{aligned} &\mathbf{M}\ddot{\mathbf{u}} + \mathbf{C}\dot{\mathbf{u}} + \mathbf{K}\mathbf{u} = \mathbf{F} \\ &\mathbf{u} = \mathbf{q} - \mathbf{q}_0 \end{aligned} \tag{3}$$

where $\mathbf{M}$, $\mathbf{C}$, $\mathbf{K}$ are the mass, damping and stiffness matrices of the catenary and $\mathbf{F}$ the external nodal force produced by the pantograph. Even though the equations have been linearised, the droppers are not able to exert compression forces, and this non-linearity has to be considered. The paper [18] proposes an efficient method for dynamic interaction with non-linear droppers, which is used in this work.

We modelled a section of the Norwegian catenary between Oslo and Eidsvoll from Pole No. 32-1 to No. 33-5, which refer to the distance from 32.04 km to 33.14 km. Additionally, the two adjacent sections are also modelled to compute the dynamic interaction in the overlapping sections. The catenary model in the static equilibrium is shown in Fig. 2, in which it has an irregular arrangement to fulfil the particular details of the track, including variable length spans, a different number of droppers in every span and different stagger values. The data necessary for modelling the catenary can be found in Appendix, which includes the mechanical properties, the mesh description, dynamic parameters and catenary topology data.

Table 1
Coefficients of the pantograph model WBL85.

D.o.f.	1	2
Stiffness	5400 N/m	0 N/m
Mass	5.2 kg	15.2 kg
Damping	40 N s/m	63.5 N s/m
Friction	0 N	7 N

2.2. Pantograph and contact model

In this work the pantograph WBL85 was modelled by a lumped mass model with two degrees of freedom and Coulomb friction (see Fig. 3). The friction was incorporated by the regulation of Coulomb law proposed by Quinn [19], which allows a continuous representation of friction. The parameters of this pantograph model can be found in Table 1. This simple model is suitable for pantograph behaviour in the 0 to 20 Hz frequency range, as required by the European Standard [20] for the validation of simulations.

The pantograph catenary interaction requires a contact model, for which we used the *penalty* contact model, which allows a certain minimal penetration between the elements in contact, the contact force f being proportional to the penetration and the contact stiffness k_{h} and zero when there is no penetration:

$$f = \begin{cases} k_{\text{h}}(z_1 - z_{\text{cw}}) & \text{if} \quad z_1 - z_{\text{cw}} > 0 \\ 0 & \text{if} \quad z_1 - z_{\text{cw}} \leq 0 \end{cases} \tag{4}$$

where z_1 is the height of the pantograph head and z_{cw} the height of the contact wire. The contact stiffness was chosen to avoid compromising precision and numerical stability. A value of $k_{\text{h}} = 100\,000$ N/m was set, which does not affect accuracy in the 0–20 Hz frequency band.

3. Validation with measurement data

The pantograph–catenary interaction contact force was measured for the same section of the catenary and pantograph modelled in this work. The train with the instrumented pantograph recorded the CF (Contact Force) at a velocity of 160 km/h. The same case was computationally simulated and the statistic values of the contact force were compared to validate the simulations.

In Fig. 4 the 20-Hz filtered contact force is represented in both the simulated interaction and the measurement. In Fig. 5 the same signals are contrasted but in the frequency domain showing an acceptable agreement. The contribution to the standard deviation of different frequency ranges is plotted in Fig. 6. The Standard [20] requires the contact force to be within certain permissible limits to validate the simulations. Table 2 shows that the simulation and experimental data satisfy the Standard [20] requirements.

Even though the measurement and the simulations fulfil the requirements of the Standard, there is still a certain misalignment. The deviation of the real catenary assembly with respect to the design data prevents the simulation from being closer to real measurements. In [21], this deviation was documented for the same catenary that is modelled in the present paper. Deviation in the longitudinal and vertical directions can result in errors in both the time and frequency domains.

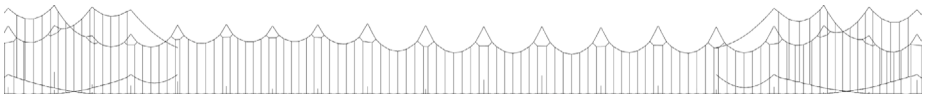

Fig. 2. Model of a section of the Oslo–Eidsvoll catenary.

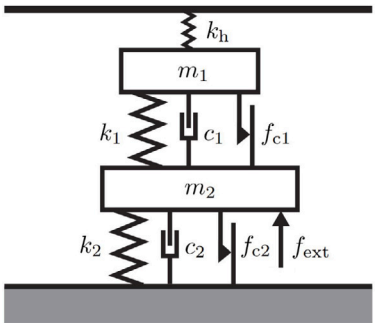

Fig. 3. Lumped mass model of the pantograph with Coulomb friction.

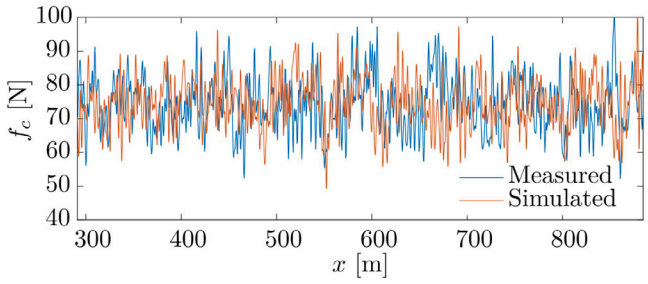

Fig. 4. Comparison of the 20-Hz filtered simulated and measured contact force.

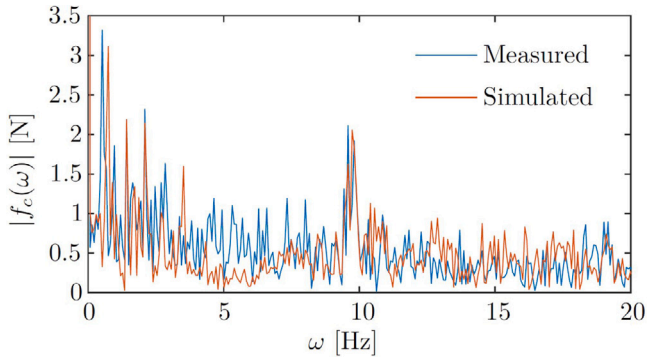

Fig. 5. Comparison of the simulated and measured contact force in the frequency domain.

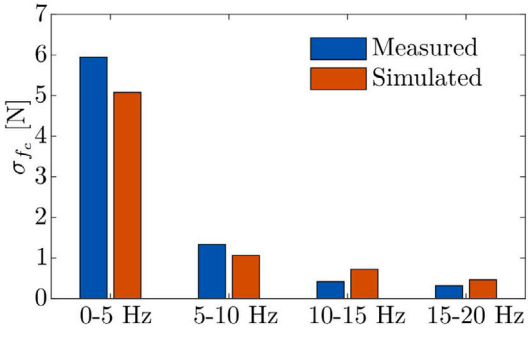

Fig. 6. Comparison of the simulated and measured contact force standard deviation.

Table 2
Validation of the contact force statistics according to [20].

	Simulated	Measured	Error	Permitted error	Pass
Mean	74.47 N	74.49 N	0.02 N	±2.5 N	Yes
Std 0–20 Hz	7.33 N	8.02 N	8.0%	±20%	Yes
Std 0–5 Hz	5.08 N	5.95 N	14.6%	±20%	Yes
Std 5–20 Hz	5.28 N	5.42 N	2.6%	±20%	Yes

4. Optimisation: proposed method

In this section, an algorithm is proposed for optimising catenary topologies, in which only parameters that have a local effect are changed in the search for better pantograph–catenary behaviour. The method is illustrated with the optimisation of the topology of a whole section of a catenary by applying changes to all the droppers in the section.

Let us say that a section of the catenary has N_d droppers and the position x_d and length l_d of every dropper d are the parameters, arranged in the vector **P**, that can be modified in the optimisation. The performance of the system is assessed by an objective function, which in this case is the standard deviation $\sigma_{f_c}(\mathbf{P})$ of the Contact Force (CF) between the pantograph and the catenary.

The optimisation problem consists of finding the value of **P** that provides the best behaviour or minimises the objective function. Unfortunately, there are too many parameters to ask any optimisation algorithm to tune all the parameters at once. The solution adopted was to optimise groups of parameters separately in multiple sub-optimisations. For this particular problem it is useful to divide the parameters into groups, since the catenary is a very large structure compared to the local effect of the parameters. A parameter influence zone (region of the catenary where the contact force is strongly affected by the parameter) does not overlap with most of the other-parameter influence zones, only with the adjacent ones. This feature is shown in Fig. 7, which shows the contact force variation produced by small modifications to the parameters (length and position) of three consecutive droppers. It can be seen that the length of every dropper affects the contact force from the previous dropper for a short distance backwards. The position of the dropper has a slightly wider influence zone, but in all cases the dropper parameter influence zones extend more backwards than forward.

The optimisation of a group of parameters (sub-optimisation) does not yield the optimum values of the global optimum, since the solution depends on the parameters with overlapping influence zones. However, in the current problem this dependence includes a small number of parameters. Taking advantage of this feature leads to an optimisation strategy that attempts to solve the coupled problem (global optimisation) by iteratively solving uncoupled problems (sub-optimisations). This strategy consists of repeating the sub-optimisations for all the groups several times in a particular order until reaching the convergence of the results.

The order in which the sub-optimisations are run is crucial for the success of the optimisation. The sub-optimisations are arranged according to the spatial position of the influence zone of the parameters on the catenary. Those that affect the contact force sooner are optimised first, so that they are ordered by their physical position according to the direction in which the train is travelling. Every time that a sub-optimisation starts, the parameters that are not being optimised adopt the value of the last sub-optimisation. When the sub-optimisations of all the groups of parameters have been carried out, the whole process is

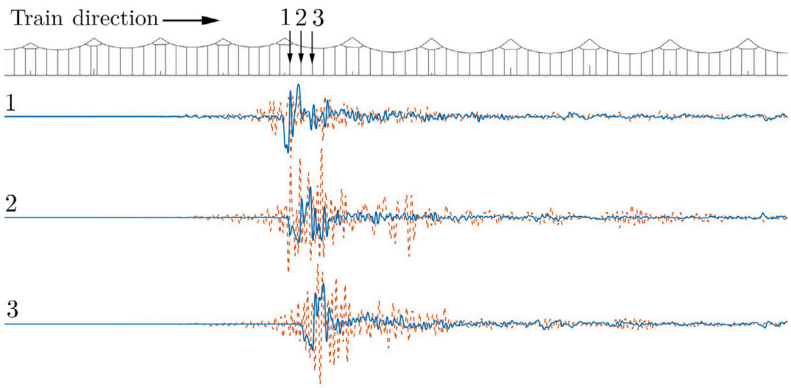

Fig. 7. Contact force variation produced by modifying the length (blue solid line) and the position (orange dashed line) of three consecutive droppers. (For interpretation of the references to colour in this figure legend, the reader is referred to the web version of this article.)

repeated in successive iterations until the improvement in the objective function is small enough, which allows the coupled effect between parameters to be considered.

The reason why the sub-optimisations are launched in the order defined by the direction the train is travelling can be understood by looking at the influence of the dropper parameters on the contact force, especially at its particular distribution as seen in Fig. 7. The influence starts slightly before the modified dropper and continues backwards while attenuating slowly. This means that the dropper d strongly affects a zone that dropper $d+1$ affects slightly. The next sub-optimisation thus cannot lose the improvement in this zone, which facilitates the parameters changing in the right direction for convergence.

The whole set of parameters $\mathbf{P}$ of the catenary is thus divided into groups of parameters, in this work every group includes the parameters of just one dropper, $\mathbf{P} = [\mathbf{p}_1 \quad \mathbf{p}_2 \quad \dots \quad \mathbf{p}_d \quad \dots \quad \mathbf{p}_{N_\mathrm{d}}]^\top$ with $\mathbf{p}_d = [x_d \quad l_d]^\top$. Therefore, the optimisation process O is divided into O_d^i sub-optimisations, being d the optimised dropper and i the iteration. For any iteration i, O_d^i for $d = 1, 2, \dots, N_\mathrm{d}$ are carried out. Groups including more parameters have shown similar solutions but higher computational costs. A smaller number of iterations is needed for bigger groups but this does not compensate for the increase in the computational cost of every sub-optimisation. This is explained because the computational cost of a sub-optimisation grows exponentially with the number of parameters, while the overall cost grows linearly with the number of sub-optimisation problems.

Every sub-optimisation process consists of the optimisation of a reduced number of parameters, in this case just the position x_d and length l_d of a dropper. The Bayesian optimisation algorithm [22] was used for all sub-optimisation, which reads as:

$$\min_{\mathbf{p}_d} \ \sigma_{f_c}(\mathbf{P}) \tag{5}$$

and the algorithm tries to minimise the function for a bounded domain of $\mathbf{p}_d$. The *bayesopt* built-in MATLAB® is implemented with an exploration ratio of 0.5. The algorithm fits a Gaussian model of the objective function and uses the model to build an acquisition function that in turn is used to determine the next evaluation point. Due to the nature of this problem with a non-smooth objective function plenty of local minima, gradient-based methods exhibit bad performance. Genetic algorithm and Bayesian optimisation are thus appropriate. However, Bayesian optimisation is more suitable for costly objective functions (as a rule of thumb more than one second) as in this case, which takes one minute approximately.

5. Optimisation results

This section describes the application of the proposed optimisation method to a particular section of the Oslo–Eidsvoll catenary (see Fig. 2), consisting of 20 spans, 16 of which are optimised (the first and last two do not affect the interaction), including $N_\mathrm{d} = 91$ droppers and twice the number of parameters (length and position of each dropper). In accordance with the Standard [20] and to evaluate the simulations, the contact force was filtered with a 20-Hz low-pass filter and the standard deviation was computed from the filtered contact force.

Every sub-optimisation O_d^i was carried out changing the parameters of dropper d for the ith iteration using the Bayesian optimisation algorithm, in which a limit of 30 evaluations was enough for the two parameters involved. Although the objective function of the global optimisation is the standard deviation of the contact force σ_{f_c} along the whole section, the objective function of the sub-optimisations was defined as the standard deviation $\sigma_{f_c}^n$ in a reduced domain around the span n, to which the optimised dropper d belongs. The selection of the domain can affect the performance of the method. Avoiding the inclusion of zones where the influence of the optimised parameters is small (see Fig. 7) can have a positive impact. The domain considered in every suboptimisation includes the span, D extra meters before and D extra meters after the span. A distant D between 20 and 30 meters has shown a better performance and therefore $D = 25$ is set in this work. This reduced domain prevents the optimisation from considering the zone in which other droppers are more significant, improving convergence and results, and also avoiding longer simulations.

The catenary was optimised for a speed of 200 km/h. The best objective function $\sigma_{f_c}^n$ achieved in every sub-optimisation is represented in Fig. 8 to show the evolution of the process. Every graph includes the results of the sub-optimisations of all the droppers (horizontal axis) of a specific span n for the different iterations (in different colours). To clarify the order in which the values or the graphs were obtained, note that every iteration starts when the previous iteration ends completely (for all the droppers in all the spans). For example, the orange curve of the first optimised span ($n = 3$) was obtained after all the blue curves were obtained. It can be seen that all the curves are necessarily decreasing and the progress of the objective function with respect to the iterations is positive and tends to converge at a value between 6 and 8 in all the spans except in the overlapping sections, where it tends towards bigger values. It should be noted that some points obtained in a specific iteration are slightly worse than in the previous iteration (e.g. in the 5th iteration of the $n = 6$ span, where the green curve is higher than the purple). This is because in that iteration the improvement achieved in previous spans led to slightly worse conditions for a specific span, but there is still a global improvement.

In Fig. 9, the objective function $\sigma_{f_c}^n$ of any span n for the final optimised catenary and the original catenary are compared, showing a great improvement. Considering the whole section, the standard deviation of the contact force is $\sigma = 15.23$ N for the original catenary and $\sigma = 7.43$ N for the optimised configuration. In Fig. 10 the 20 Hz-filtered contact force is also compared for both configurations, showing the reduction in the oscillation amplitude of the optimised result. The

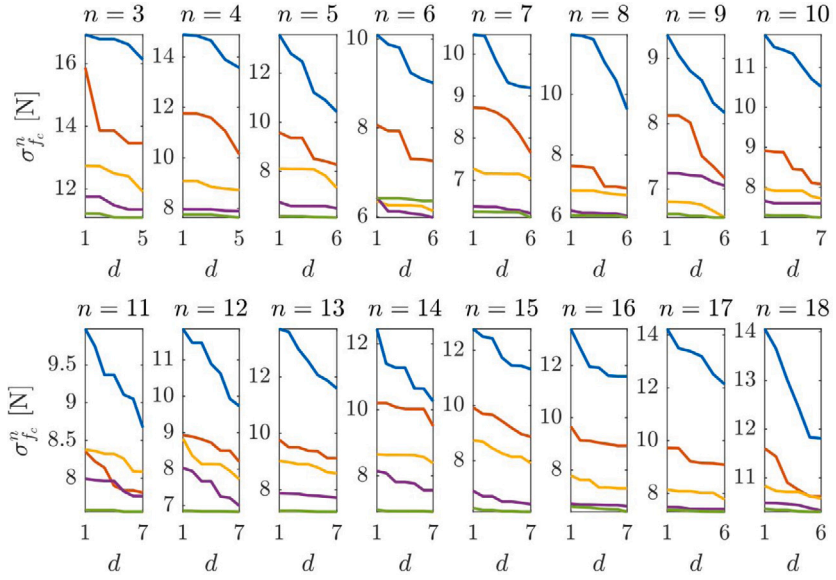

Fig. 8. Evolution of the optimisation process. Standard deviation $\sigma^n_{f_c}$ of span n after every sub-optimisation O^i_d of dropper d at iteration i. $i = 1$ blue, $i = 2$ orange, $i = 3$ yellow, $i = 4$ purple and $i = 5$ green. (For interpretation of the references to colour in this figure legend, the reader is referred to the web version of this article.)

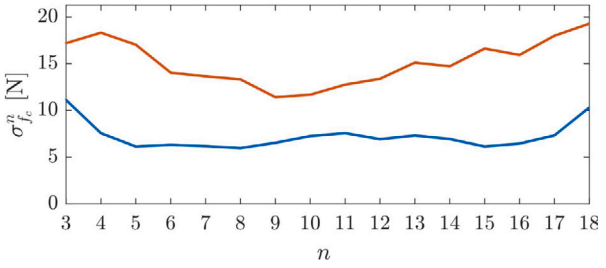

Fig. 9. Standard deviation of the n span of the original (orange) and optimised (blue) catenaries. (For interpretation of the references to colour in this figure legend, the reader is referred to the web version of this article.)

configuration of the contact wire before and after the optimisation is shown in Fig. 11. The optimised solution does not exhibit symmetry nor periodicity and the characteristics of the solution depend on every specific problem.

As said above, this method allows the optimisation of a catenary section that with a conventional approach is unaffordable. Taking into account the cost of the objective function (about 1 min with a 12th Gen Intel®Core(TM) i9-12900KS 3.40 GHz) and the fact that gradient-based methods are not appropriate for this problem, the inclusion of 180 parameters in a single optimisation is far from being feasible. On the contrary, with the proposed approach the optimisation takes 900 evaluations per span, lasting about 15 h that can be reduced to 2 h with the advantage of parallel computing (12 workers).

5.1. Different scenarios

The optimisation described above was conducted for a speed of 200 km/h, which is the line operational speed for passenger trains. However, the trains also operate at different speeds, e.g. goods trains travel at 160 km/h on the same track, and different pantographs can be used with the same catenary. In this subsection, the optimised catenary was tested at 160 and 200 km/h with the WBL85 (used for the optimisation) and WBL88 (Table 3) pantographs. The catenary was also optimised for a speed of 160 km/h and tested for both speeds and both pantographs. The standard deviation of the 200 km/h-optimised catenary is compared with the original one in Table 4.

Table 3
Coefficients of the pantograph model WBL88.

D.o.f.	1	2
Stiffness	4400 N/m	0 N/m
Mass	6.6 kg	19.76 kg
Damping	75.6 N s/m	63.5 N s/m

Table 4
Standard deviation change from the original catenary to the optimised catenary at 200 km/h.

Pantograph	WBL85[a]	WBL88
200 km/h[a]	15.23 N → 7.43 N (−51%)	18.66 N → 9.36 N (−50%)
160 km/h	10.48 N → 11.73 N (+11%)	11.49 N → 13.38 N (+16%)

[a] Speed and pantograph set for the optimisation.

Table 5
Standard deviation change from the original catenary to the optimised catenary at 160 km/h.

Pantograph	WBL85[a]	WBL88
200 km/h	15.23 N → 14.27 N (−6%)	18.66 N → 17.29 N (−7%)
160 km/h[a]	10.48 N → 6.59 N (−37%)	11.54 N → 7.71 N (−33%)

[a] Speed and pantograph set for the optimisation.

The improvement achieved in the optimisation still remains with the WBL85 pantograph. However, the optimised catenary does not perform better for the different speed, for any of the pantographs. Similar results were achieved for the 160 km/h-optimised catenary. As summarised in Table 5, a vast improvement was found at 160 km/h (optimisation speed) while the improvement is quite small at 200 km/h.

Given the optimised catenaries lack of significant improvement when operated at different speeds from those set in the optimisations, we conducted a new optimisation in which the objective function is the mean of the standard deviation at 160 and 200 km/h within the sub-optimisation domain, $\sigma^n_{f_c} = 0.5(\sigma^n_{f_c(160\ \mathrm{km/h})} + \sigma^n_{f_c(200\ \mathrm{km/h})})$. Table 6 gives the results of the optimised catenary at both speeds compared with the original catenary. In this case the improvement is obtained at both speeds, reducing the standard deviation to around 20% at 160 km/h and a 35% at 200 km/h, which are lower than the 35% and 50% obtained at 160 and 200 km/h single speed optimisations. The optimised catenary was also tested at 170, 180 and 190 km/h, showing

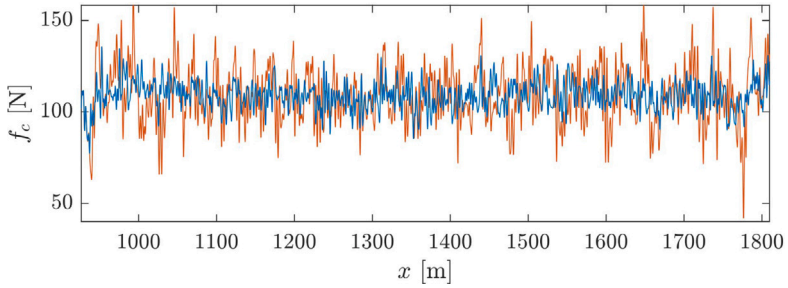

Fig. 10. 20 Hz filtered contact force of the original (orange) and optimised (blue) catenaries. (For interpretation of the references to colour in this figure legend, the reader is referred to the web version of this article.)

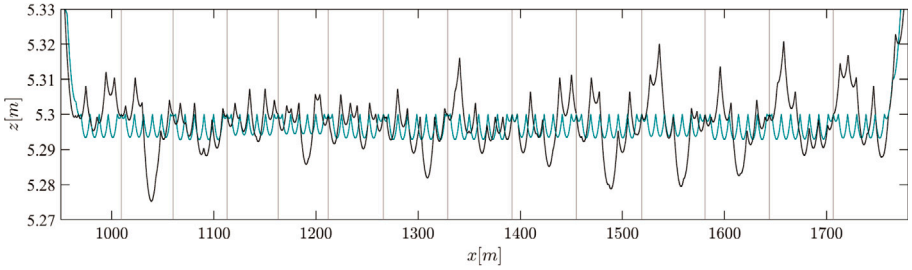

Fig. 11. Contact wire geometry before (green) and after (black) the optimisation. Spans are delimited with the vertical lines. (For interpretation of the references to colour in this figure legend, the reader is referred to the web version of this article.)

Table 6
Standard deviation change from the original catenary to the optimised catenary at 160 and 200 km/h.

Pantograph	WBL85[a]	WBL88
160 km/h[a]	10.48 N → 8.29 N (−21%)	11.54 N → 9.40 N (−19%)
170 km/h	12.42 N → 9.65 N (−16%)	12.85 N → 10.83 N (−16%)
180 km/h	13.38 N → 10.70 N (−20%)	14.36 N → 12.34 N (−14%)
190 km/h	14.43 N → 10.97 N (−24%)	16.74 N → 12.92 N (−23%)
200 km/h[a]	15.23 N → 9.65 N (−37%)	18.66 N → 12.21 N (−35%)

[a] Speed and pantograph set for the optimisation.

a significant improvement for those speeds which were not included in the optimisation.

6. Conclusions

This work aimed to optimise the catenary topology by modifying the dropper positions and lengths (although the proposed method could be applied using other features) to reduce the standard deviation of the pantograph–catenary contact force and have a better current collection quality. The optimisation was set for a real catenary design scenario in which there is no periodicity and the catenary topology varies along the track. In this scenario, the definition of the topology relies on a vast number of parameters, which makes the computational cost unaffordable. However, these circumstances are found in the general catenary layouts, so that an optimisation strategy is needed to deal with this challenge for a proper design.

To cope with the large number of optimisation parameters, we proposed a method that divides these parameters and performs multiple recursive sub-optimisations. The idea is based on the fact that n optimisations of one nth of the number of optimisation parameters are very much faster than one optimisation including all of them. This method takes advantage of the large size of the catenary and therefore the weak interdependence of most of the optimisation parameters. The method proved to be successful in reducing the objective function significantly, and although it does not ensure the absolute minimum, it provides a compromise solution with a good improvement and feasible computational cost.

A different matter is the robustness of the optimisation, i.e. whether the improvement achieved for certain operating conditions remains when these conditions are changed. In this paper, the optimised catenaries were tested at different speeds and pantographs from those used in the optimisations, showing that a catenary optimised for a specific speed does not give a better performance at a different speed. An optimisation was thus carried out that sought the solution that had a better average performance at two different speeds, leading to a smaller improvement but with more robust results.

CRediT authorship contribution statement

J. Gil: Conceptualization, Methodology, Investigation, Software, Writing – original draft. **Y. Song:** Supervision, Resources. **S. Gregori:** Software, Validation, Visualization. **M. Tur:** Supervision, Funding acquisition. **A. Rønnquist:** Supervision, Project administration. **F.J. Fuenmayor:** Conceptualization, Project administration.

Declaration of competing interest

The authors declare that they have no known competing financial interests or personal relationships that could have appeared to influence the work reported in this paper.

Data availability

The authors are unable or have chosen not to specify which data has been used.

Acknowledgements

The authors would like to acknowledge the financial support received from the State Research Agency of the Spanish Science and Innovation Ministry, Spain (PID2020-113458RB-I00) and from the Valencian Regional Government, Spain (PROMETEO/2021/046).

Table A.7
Positions of messenger and contact wire support points.

Pole	x [m]	y [m]	z cw [m]	z mw [m]
1	0	0	5.8	6.5
2	54.4	−0.16	5.8	7.52
3	104.4	−0.15	5.45	7.6
4	145.4	−0.15	5.3	6.81
5	187.4	0.3	5.3	6.85
6	238	0.15	5.3	7.08
7	291	0.3	5.3	7.1
8	341	−0.3	5.3	7.06
9	390	0.3	5.3	7.09
10	444	−0.3	5.3	7.12
11	507	0.2	5.3	7.07
12	570	−0.3	5.3	7.04
13	633	−0.22	5.3	7.04
14	697	0.3	5.3	7.02
15	759	−0.25	5.3	7.06
16	822	0.25	5.3	7.03
17	884.6	−0.3	5.3	7.06
18	938.6	0.3	5.3	7.07
19	987.6	0.15	5.45	7.56
20	1039.6	0.75	5.8	7.48
21	1099	0	5.8	6.5

Table A.8
Dropper spacing: distance between droppers or between dropper and steady arm. Stitch wire spacing: distance between the start/end point of the stitch wire and the steady arm.

Span	Dropper spacing								Stitch wire	
	1	2	3	4	5	6	7	8	1	2
2	9.2	9.2	9.2	9.2	9.2	4				
3	4	8.63	8.63	8.63	8.63	2.48				7
4	2.5	8.88	8.88	8.88	8.88	3.98			7	7
5	4	8.82	8.82	8.82	8.82	8.82	2.5		7	7
6	2.5	9.3	9.3	9.3	9.3	9.3	4		7	7
7	4	8.4	8.4	8.4	8.4	8.4	4		7	7
8	4	8.2	8.2	8.2	8.2	8.2	4		7	7
9	4	9	9	9	9	9	5		7	9
10	5	9.25	9.25	9.25	9.25	9.25	9.25	2.5	9	9
11	2.5	9.25	9.25	9.25	9.25	9.25	9.25	5	9	9
12	5	8.83	8.83	8.83	8.83	8.83	8.83	5.02	9	9
13	5	9	9	9	9	9	9	5	9	9
14	5	8.67	8.67	8.67	8.67	8.67	8.67	4.98	9	9
15	5	9.25	9.25	9.25	9.25	9.25	9.25	2.5	9	9
16	2.5	9.18	9.18	9.18	9.18	9.18	9.18	5.02	9	9
17	5	9	9	9	9	9	4		9	7
18	4	8.2	8.2	8.2	8.2	8.2	4		7	
19	4	9.6	9.6	9.6	9.6	9.6				

Appendix. Modelling data

This appendix provides additional data for modelling the catenary section studied of a section of the Norwegian catenary between Oslo and Eidsvoll from Pole No. 32–1 to No. 33–5, from 32.04 km to 33.14 km.

Table A.7 gives the coordinates of the contact wire and messenger wire support points. Note that the x and y coordinates are the same for both wire support points.

Table A.8 gives the horizontal distances between consecutive droppers (or between a dropper and the adjacent steady arm) of all spans. The stitch wire is defined by two distances: the horizontal distance between the first pole of the span and the end point of the stitch wire, and the horizontal distance between the starting point of the stitch wire and the last pole in the span. Table A.8 gives both distances for every span in the section.

The mechanical properties of the elements are given in Table A.9. Note that the elements modelled with beam type element have second area moment I, whereas those modelled with bar type element do not.

The clamps used to fasten the wires are modelled with point masses. The droppers are attached to the contact, messenger and stitch wires with 0.105 kg clamps. The messenger wire and the stitch wires are connected with 0.38 kg clamps, while the steady arms pull the contact wire through 0.278 kg clamps.

Table A.9
Mechanical properties of the elements.

Element	Young modulus (GPa)	Area (mm^2)	Density (kg/m^3)	I (mm^4)
Messenger wire	108	65.8	9058	344.5
Contact wire	120	120	8917	1145.9
Droppers	103	9.7	8786	–
Stitch wire	108	33.4	9012	–
Steady arm	0.13	923.6	498	–

The messenger and contact wire tension is set to 1500 N, while the stitch wire to 2800 N.

The average length of contact wire elements is 0.2 m, while in the messenger and stitch wires it is 0.6 m.

The integration method used is the HHT (Hilber Hughes Taylor) [23]. The coefficients related to the method are summarised in Table A.10. The Rayleigh damping model is considered, in which the damping matrix is proportional to the mass and stiffness matrices, $\mathbf{C} = \alpha_r \mathbf{M} + \beta_r \mathbf{K}$. Being the coefficients $\alpha_r = 0.062\ s^{-1}$ and $\beta_r = 6.1310^{-6}$ s.

Table A.10
Coefficients for the HHT integration method.

Δt (s)	α	γ	β
0.001	−0.05	0.5	0.25

References

[1] Bruni S, Bucca G, Carnevale M, Collina A, Facchinetti A. Pantograph–catenary interaction: recent achievements and future research challenges. Int J Rail Transp 2018;6(2):57–82. http://dx.doi.org/10.1080/23248378.2017.1400156.

[2] Bruni S, Ambrosio J, Carnicero A, Cho YH, Finner L, Ikeda M, Kwon SY, Massat JP, Stichel S, Tur M. The results of the pantograph-catenary interaction benchmark. Veh Syst Dyn 2015;53(3):412–35. http://dx.doi.org/10.1080/00423114.2014.953183.

[3] Zhou N, Zhang W. Investigation on dynamic performance and parameter optimization design of pantograph and catenary system. Finite Elem Anal Des 2011;47(3):288–95. http://dx.doi.org/10.1016/j.finel.2010.10.008.

[4] Cho YH, Lee K, Park Y, Kang B, nam Kim K. Influence of contact wire pre-sag on the dynamics of pantograph–railway catenary. Int J Mech Sci 2010;52(11):1471–90. http://dx.doi.org/10.1016/j.ijmecsci.2010.04.002, URL https://www.sciencedirect.com/science/article/pii/S0020740310000998, Special Issue on Non-linear Oscillations.

[5] Yu M, Liu W, Zhang J, Yan C. Influence of dropper spacing on quality of pantograph-catenary current collection. Appl Mech Mater 2014;654:78–81. http://dx.doi.org/10.4028/www.scientific.net/AMM.654.78.

[6] Mengzhen W, Xianghong X, Yongzhao Y, Yi L, Sijun H, Jianshan W. Multi-parameter joint optimization for double-strip high-speed pantographs to improve pantograph-catenary interaction quality. Acta Mech Sin 2022;38(521344). http://dx.doi.org/10.1007/s10409-021-09018-x.

[7] Massat J-P, Laurent C, Bianchi J-P, Balmès E. Pantograph catenary dynamic optimisation based on advanced multibody and finite element co-simulation tools. Veh Syst Dyn 2014;52(sup1):338–54. http://dx.doi.org/10.1080/00423114.2014.898780.

[8] Koziel S, Yang X, editors. Computational optimization, methods and algorithms. In: Computational optimization, methods and algorithms. Studies in computational intelligence, vol. 356, 2011, p. 1–281. http://dx.doi.org/10.1007/978-3-642-20859-1.

[9] Burczynski T, Kus W, Beluch W, Dlugosz A, Poteralski A, Szczepanik M. Structural intelligent optimization. In: Intelligent computing in optimal design. Solid mechanics and its applications, vol. 261, 2020, p. 77–195. http://dx.doi.org/10.1007/978-3-030-34161-9_4.

[10] Nåvik P, Rønnquist A, Stichel S. The use of dynamic response to evaluate and improve the optimization of existing soft railway catenary systems for higher speeds. Proc Inst Mech Eng F 2016;230(4):1388–96. http://dx.doi.org/10.1177/0954409715605140.

[11] Zhang J, Liu W, Zhang Z. Sensitivity analysis and research on optimisation methods of design parameters of high-speed railway catenary. IET Electr Syst Transp 2019;9(3):150–6. http://dx.doi.org/10.1049/iet-est.2018.5007.

[12] Gregori S, Tur M, Nadal E, Fuenmayor FJ. An approach to geometric optimisation of railway catenaries. Veh Syst Dyn 2018;56(8):1162–86. http://dx.doi.org/10.1080/00423114.2017.1407434.

[13] Wang H, Zheng D, Huang P, Yan W. Design optimisation of railway pantograph-catenary systems with multiple objectives. Veh Syst Dyn 2022;1–23. http://dx.doi.org/10.1080/00423114.2022.2151921.

[14] Su K, Zhang J, Zhang J, Yan T, Mei G. Optimisation of current collection quality of high-speed pantograph-catenary system using the combination of artificial neural network and genetic algorithm. Veh Syst Dyn 2023;61(1):260–85. http://dx.doi.org/10.1080/00423114.2022.2045029.

[15] Gregori S, Gil J, Tur M, Tarancón J, Fuenmayor F. Analysis of the overlap section in a high-speed railway catenary by means of numerical simulations. Eng Struct 2020;221:110963. http://dx.doi.org/10.1016/j.engstruct.2020.110963.

[16] Berzeri M, Shabana A. Development of simple models for the elastic forces in the absolute nodal co-ordinate formulation. J Sound Vib 2000;235(4):539–65. http://dx.doi.org/10.1006/jsvi.1999.2935.

[17] Tur M, García E, Baeza L, Fuenmayor F. A 3D absolute nodal coordinate finite element model to compute the initial configuration of a railway catenary. Eng Struct 2014;71:234–43. http://dx.doi.org/10.1016/j.engstruct.2014.04.015.

[18] Gregori S, Tur M, Nadal E, Aguado JV, Fuenmayor FJ, Chinesta F. Fast simulation of the pantograph–catenary dynamic interaction. Finite Elem Anal Des 2017;129:1–13. http://dx.doi.org/10.1016/j.finel.2017.01.007.

[19] Quinn DD. A new regularization of Coulomb friction. J Vib Acoust 2004;126(3):391–7. http://dx.doi.org/10.1115/1.1760564.

[20] EN 50318:2018. Railway applications. Current collection systems. Validation of simulation of the dynamic interaction between pantograph and overhead contact line. European Committee for Electrotechnical Standardization; 2018.

[21] Song Y, Jiang T, Nåvik P, Rønnquist A. Geometry deviation effects of railway catenaries on pantograph–catenary interaction: a case study in Norwegian Railway System. Railw Eng Sci 2021;29. http://dx.doi.org/10.1007/s40534-021-00251-0.

[22] Mockus J. The Bayesian approach to local optimization. In: Bayesian approach to global optimization: Theory and applications. Dordrecht: Springer Netherlands; 1989, p. 125–56. http://dx.doi.org/10.1007/978-94-009-0909-0_7.

[23] Hilber HM, Hughes TJ, Taylor RL. Improved numerical dissipation for time integration algorithms in structural dynamics. Earthq Eng Struct Dyn 1977;5(3):283–92. http://dx.doi.org/10.1002/eqe.4290050306.